^{63}Cu NMR studies of copper sulfide

Shin-hachiro Saito, Hideki Kishi,* Kohji Nié,† and Hisakazu Nakamaru
Physics Laboratory, Faculty of Engineering, Toin University of Yokohama, Kurogane-cho 1614, Aoba-ku, Yokohama 225, Japan

Fumihiko Wagatsuma and Takeshi Shinohara
Institute for Materials Research, Tohoku University, Katahira 2-1-1, Aoba-ku, Sendai 980-77, Japan
(Received 8 August 1996; revised manuscript received 26 December 1996)

We have measured the ^{63}Cu NMR of powdered copper sulfide CuS, in the region between 1.5 K and a room temperature, under magnetic field up to 6.5 T. An intense resonance peak and its satellites have been observed at all of the measured temperatures. The intense peak consists of two resonance lines above 60 K, and four lines below about 50 K. The splitting corresponds to the reported crystalline distortion and anomaly in specific heat below 55 K. There are complex satellites around the central intense peak, which are attributable to the first- and second-order quadrupole splittings. The Knight shifts of the central intense peak are nearly temperature independent and range from 0.04 to 0.16 % in the region between 1.6 K and a room temperature. The central peak and the observed satellites can be assigned to the metallic Cu(1) and less metallic Cu(2) in the crystalline structure of CuS. An anomalous negative Knight shift is estimated for the metallic Cu(1). The spin-lattice relaxations times, T_1 have also been measured for both the Cu(1) and Cu(2) nuclei. T_1 for Cu(2) nuclei is about 55 ms at 15 K, while that for Cu(1) nuclei is anisotropic and anomalously short 4 ms at 15 K, which suggests the metallic character in the plane formed by Cu(1)-S bonds. [S0163-1829(97)05621-X]

I. INTRODUCTION

Since 1929, it has been known that copper sulfide CuS, condenses into the superconducting state below near 1.6 K,[1,2] and the reason could not be explained why the superconductivity appears in CuS, although the constitutive elements both Cu and S do not condense into this state.

After the discovery[3] of high-T_c copper-oxide superconductors, it became possible to have a conjecture for the mechanism of superconductivity of CuS through an analogy between Cu-O and Cu-S bonds. Sulfur, S_{16}, belongs to the same group as oxygen in the Periodic Table and its electronic configuration of the outer shell of the atom is $3s^2 3p^4$, while that of O_8 is $2s^2 2p^4$.

Furthermore, recent investigations of the high-T_c copper-oxide superconductors have revealed that the electronic holes in Cu-O layers of these oxides play an important role in the appearance of superconductivity. In practical use, however, the copper-oxide superconductors still have some weaknesses which come from the poor carrier density, the short coherence length, the rise of electric resistivity in an applied magnetic field, and so on.

Our motivation for the present study is to clarify the difference between the superconductivity due to Cu-O and Cu-S bonds, and to seek better characteristics caused by the use of Cu-S layers than that of Cu-O layers.

In this paper, ^{63}Cu NMR has been observed and analyzed for the microscopic studies of electric and magnetic properties of the Cu-S bond in CuS. The measurements reveal that ^{63}Cu NMR in CuS consists of a central intense peak and its satellites and that Knight shifts of the central intense peak range from 0.04 to 0.16 %, and are nearly constant through the temperature region above T_c.

An analysis of the satellites on both sides of the central intense peak shows that there exist first- and second-order quadrupolar interactions between Cu nuclei and their surrounding electric-field gradients (EFG). The second-order quadrupolar interaction and negative Knight shift are estimated for Cu(1) nuclei.

An anisotropic relaxation has been observed for the second-order quadrupolar satellites. This is of particular interest for the metallic Cu(1)-S plane.

The influence of crystalline state on superconducting transition has also been studied referring to the results of x-ray diffraction. The experimental facts suggest that growth of crystalline planes plays an important role in the appearance of superconductivity. From the measurement of ac magnetic susceptibilities χ' and χ'', an anisotropic χ'' behavior has been observed in the c-axis-orientated CuS samples.

II. CRYSTAL STRUCTURE AND SPECIFIC HEAT

The crystal structure of CuS was investigated by many authors.[4–6] CuS has hexagonal structure at 295 K, which is shown in Fig. 1(a).[6] The slight distortion and atomic displacements take place below about 55 K, which is shown in Fig. 1(b).[6] There are two sites of the Cu atom at the temperature above 55 K, as shown in Fig. 1(a), where Cu(1)'s lie in the plane triangularly coordinated by S atoms, which have the Cu-S bond length 2.17–2.19 Å, and Cu(2)'s are tetrahedrally coordinated by S atoms, which have the Cu-S bond length 2.28–2.33 Å. The triangularly coordinated Cu(1) plane is almost perpendicular to the c axis. Therefore, the growth of x-ray diffraction lines[4] (002), (004), (006), and (008) means relative formation of the plane including Cu(1).

The low-dimensional character of this substance has already been pointed out in the specific-heat measurement by Isino and Kanda,[7] and Westrum, Stolen, and Gronveld.[8] They reported that the lattice specific heat of CuS did not

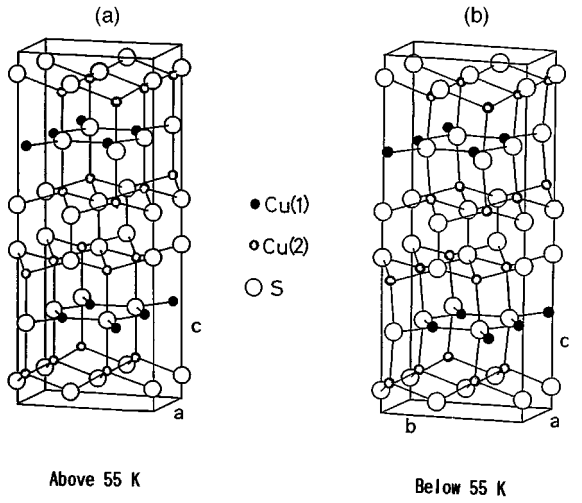

FIG. 1. Crystal structure of CuS, reported in Ref. 6. Cu(1) atoms (solid circles) lie in the plane triangularly coordinated by S atoms, and Cu(2) atoms (open circles) are tetrahedrally coordinated by S atoms. (a) Temperature at 295 K. Orthohexagonal setting. (b) Temperature below 50 K. Slight distortion of (a).

obey the T^3 law, but rather T^2 in the temperature region below about 20 K. They assumed a quasi-two-dimensional lattice and that the anomaly might originate from the weak bonding in the direction of the c axis. Ishino and Kanda[7] pointed out that CuS might be an anisotropic superconductor.

III. EXPERIMENTS

A. Samples

Two sources for the CuS sample have been used. One (''sample W'') was commercially obtained from chemical reagent companies, and the other (''sample Sy'') was synthesized in our laboratory.

The CuS samples obtained from a few companies have been examined by means of the x-ray diffraction. The sample has been pulverized to fine powder in an agate mortar, then sieved with sieve of 200 mesh, and powders of diameter smaller than 75 μm have been mounted to the cell in x-ray-diffraction apparatus. The diffraction pattern for the sample, supplied by Wako-pure-chemical industries Ltd., has been able to fit with the reported result,[4] which we have named sample W. However, sample W did not show the superconductivity down to 1.2 K, which was the lowest temperature attained in the present measurement.

The chemical stoichiometry of sample W measured by x-ray fluorescence analysis was $Cu_{1.17}S$ within errors of 6%. The superconductivity for this reagent has been detected after annealing in an electric oven for 1 h at 400 °C. The superconducting transition temperature T_c has been determined with an ac mutual inductance bridge (Hartshorn bridge). The temperature at the beginning of mutual inductance change (χ' in $\chi=\chi'+i\chi''$) has been defined as nominal T_c (onset). The x-ray-diffraction pattern of the delivered powder, sample W, which does not show the superconductivity, is shown in Fig. 2(a). After annealing of the sample W at 400 °C for 1 h, the superconducting transition has been observed at 1.60 K. The diffraction pattern of the baked sample W is shown in

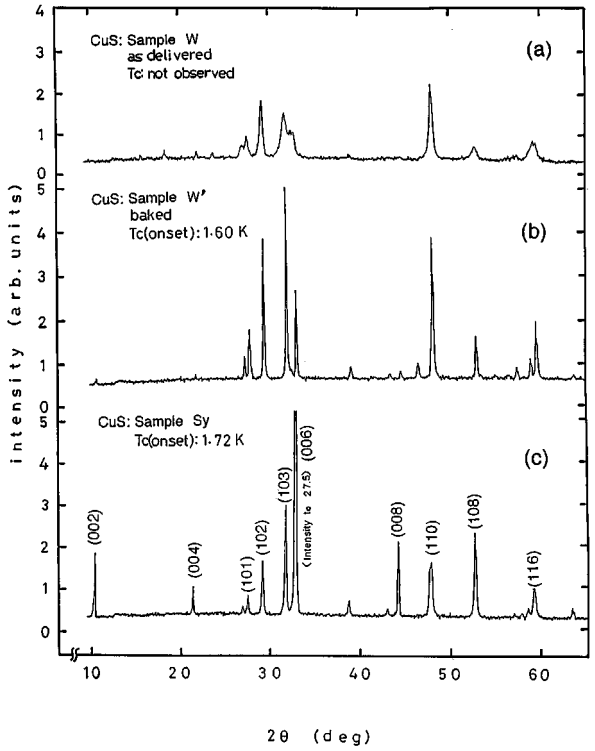

FIG. 2. X-ray-diffraction patterns of CuS. (a) Commercially delivered CuS, named sample W. (b) The sample W', which is baked sample W during 1 h at 400 °C. (c) The sample Sy, synthesized in our laboratory.

Fig. 2(b) named sample W'. The measured molar stoichiometry for the sample W' is $Cu_{1.14}S$. There are no essential differences between Figs. 2(a) and 2(b), but line shapes in Fig. 2(b) are rather sharp and small additional lines assigned to (002), (004), and (008) are observed. This may be explained by progressive growth of crystal structure in sample W'.

For sample Sy, we prepared CuS samples ourselves starting from purified sulfur and a high-purity copper bar of five nines. The purification of sulfur was made by the recrystallization of sulfur from a CS_2 solution. A copper bar of 1 mm diameter and purified sulfur were sealed in a Pyrex glass tube and annealed at 500 °C in an electric oven for 110 h. T_c of the synthesized sample, named sample Sy, has been observed at 1.72 K, and the stoichiometry measured as $Cu_{1.02}S$ from the x-ray fluorescence analysis.

Figure 2(c) shows the x-ray-diffraction pattern for the sample Sy, where we can see that the intensities of lines (002), (004), (006), and (008) are relatively higher than those of Fig. 2(b). From the results shown in Figs. 2(a), 2(b), and 2(c), we confirm here that the crystalline state of CuS plays an important role in determining the superconducting behavior.

B. Anisotropic imaginary magnetic susceptibility χ'' of superconducting CuS

Practical knowledge with regard to the Meissner effect and power dissipation of a bulk superconductor are often obtained by the measurements of ac complex magnetic

susceptibilities[9,10] in the transition temperature region. Especially, the imaginary part χ'' of ac magnetic susceptibility is one of the sensitive probes for power dissipation and screening in the filamentary structure[11] of a superconductor or in the weak link[12] inside of the bulk specimen. This type of work has done much for the high-T_c superconductor. To clarify the superconducting mechanism in CuS, it may be contributory to study the anisotropy of χ'' in CuS as an analogy between Cu-O and Cu-S bonds.

In the present work, we have prepared the c-axis-orientated CuS sample, starting from the purified sulfur and strips of stretched high-purity copper wire. In the stretched copper wire of diameter 1 to 3 mm, the longitudinal direction is mostly orientated to direction parallel to the crystalline c axis, but not orientated in the plane perpendicular to the c axis. Sulfurating the stretched wire, we obtained the c-axis-orientated CuS. The orientation in the synthesized specimen has been discriminated by x-ray diffraction, comparing the planes (004), (006), and (008) which are perpendicular to the c axis. Two spheroidal shaped samples have been cut from the synthesized cylindrical specimen as shown in the inset of Fig. 3, which have mutually perpendicular axes and nearly equal volumes and weights 0.040 $\pm$0.001 g. The complex ac magnetic susceptibility has been measured with a mutual inductance bridge. The imaginary part χ'' has been measured as the variation of a phase-regulating potentiometer. As the samples were immersed in superfluid He II, the homogeneity of temperature in the specimens was fairly good.

The χ' and χ'' results are given in Fig. 3. The differences between the χ' for the normal state and that for the superconducting state are nearly equal for both samples $\perp c$ and $\| c$, while the χ'' for $\perp c$ is about two times larger than for $\| c$. These results could be explained by the larger power dissipation in the plane perpendicular to the c axis, in which the electric conductivity is larger than that in the direction parallel to the c axis.

An anisotropic electric conductivity of CuS has separately been measured by the four-terminal method. The obtained results are shown in Table I. The measurement below 77 K failed because of the higher conductivity of sample and of the difficulty in keeping a stable contact of leads to the anisotropic specimens. From room temperature down to 77 K, however, we have observed the anisotropic behavior in the electrical conductivity of CuS.

C. ^{63}Cu NMR: Temperature dependence

A conventional phase-coherent pulsed NMR apparatus has been used for ^{63}Cu NMR study under magnetic fields between about 3 and 6 T. Knight shifts have been measured both from the echo intensity as a function of magnetic field, and from power spectra of fast Fourier transform (FFT) of free-induction decays as a function of frequency. The shifts have been referenced to the ^{63}Cu FFT spectrum in CuBr as a standard substance.

The whole envelope of echo intensities as a function of magnetic field for the sample Sy at a room temperature are shown in Fig. 4. The 90° pulse width of 20 μ s and 90°–180° pulse separation of 200 μ s have been used in the measurement.

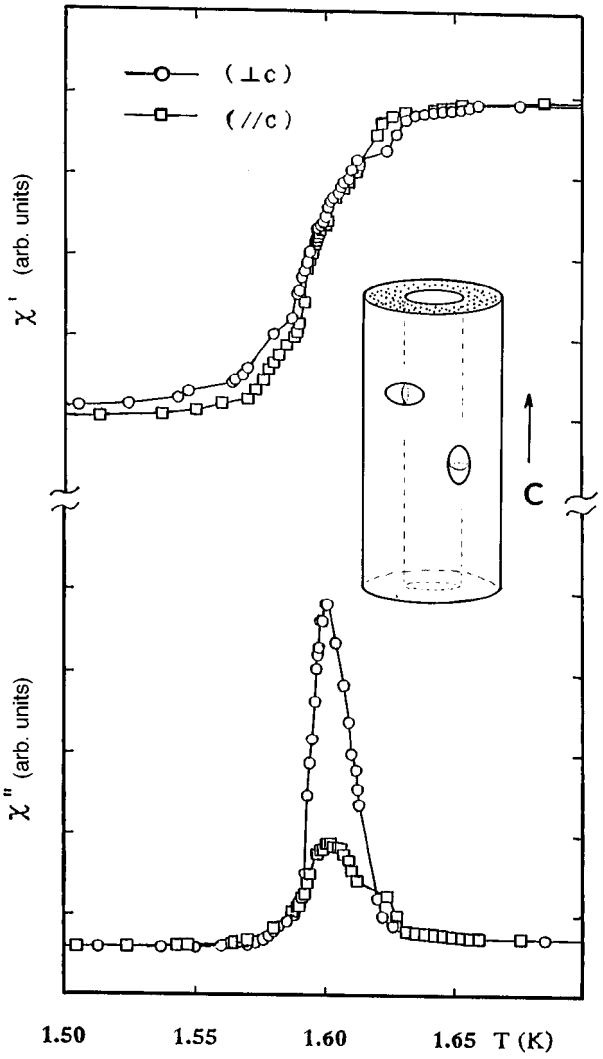

FIG. 3. Anisotropic complex ac magnetic susceptibility, χ' and χ'' of c-axis-orientated CuS as a function of temperature. Inset shows the cutting out of the spheroidal samples from the cylindrical specimen. Upper sample has an anisotropic direction perpendicular $\perp$ c axis, and lower one $\| c$.

The intense central peaks at 15 K are shown in Figs. 5(a) and 5(b) of the sample W and the sample Sy, respectively. The spectrum for the sample W is broad and the splitting is not clear even at 15 K, as shown in Fig. 5(a), while that for the sample Sy split into two peaks as shown in Fig. 5(b) and remains still two peaks in the higher temperature region above 55 K as shown in Fig. 5(c). In the region below about 50 K, it seems that the peak does not change largely, but distinguishable shoulders appear on both sides of the echo intensity as shown in Fig. 5(b), where these shoulders are

TABLE I. Anisotropies of electric resistivity ρ in c-axis-orientated CuS.

	$\rho_{\| C}$ (Ω m)	$\rho_{\perp C}$ (Ω m)	$\rho_{\| C}/\rho_{\perp C}$
Room temperature	3.61×10^{-6}	6.03×10^{-7}	5.99
Liq. N_2 (77 K)	8.05×10^{-7}	1.31×10^{-7}	6.15

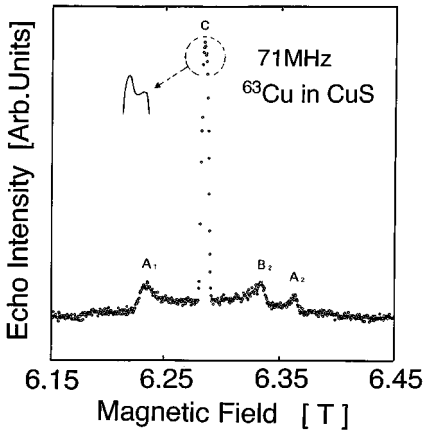

FIG. 4. The whole envelope of ^{63}Cu NMR echo intensity for the sample Sy at 295 K as a function of magnetic field between 6.2 and 6.5 T. The radio frequency 71 MHz, was used.

shown by arrows. These shoulder components have been confirmed by the power spectra of FFT at 15 K, which are shown in Figs. 6 and 7. In the low-temperature region below 50 K, the resolutions of FFT spectra are rather clearer than that of the echo intensities as a function of magnetic field. The FFT spectra consist of four components of resonance. In Fig. 6, the position of the excitation frequency near the resonance is shown by arrow. It is evident that the excitation by 90° pulse at the frequency rather distant from the resonance gives good resolution for the power spectra. Every resolution in Fig. 6 shows that the spectra consists of four peaks, except for the case of excitation frequency $f=71.528$ MHz, and that the total envelope of power spectra range over 150 KHz from 71.48 to 71.63 MHz. As shown in the middle of Fig. 6, the excitation at the frequency, $f=71.528$ MHz, which is the inside of the resonance line shape, leads to a partial lack of power spectrum. In this case, the power spectrum consists of not four peaks but two peaks. The FFT power spectra of the central intense peak for the sample Sy as a function of temperature are shown in Fig. 7, where the spectra split into four components below 50 K, although the lowest frequency component is out of the figure.

As shown in Figs. 5(b), 5(c), and 6, ^{63}Cu resonances of the central peak consist of four components in the region below 50 K, and two components in the region above 55 K. This change of spectrum from room temperature to below 50 K corresponds to the reported crystalline deformation,[6] and the anomalies in specific heat[8] and Hall coefficient.[13]

The splitting in the FFT power spectra and echo intensity are plotted in Fig. 8 as the temperature dependence of Knight shift %. The Knight shift ranged from 0.04 to 0.16 %, and is almost temperature independent, showing the metallic character of the central intense peak.

When the magnetic field is lowered, the detailed profile of the peak is modified as shown in Fig. 9, where the higher peak under the field 6.30 T goes to the lower peak under the field 3.32 T. If we measure, however, the Knight shift $\Delta H/H$ of each line, we can see that the shifts, %, do not change for both lines of the doublet. Furthermore, the distance of two peaks of C is about 50 G under the applied field 6 T, as shown in the upper part of Fig. 9, while it is about 25 G under the applied field 3 T as shown in the lower part of

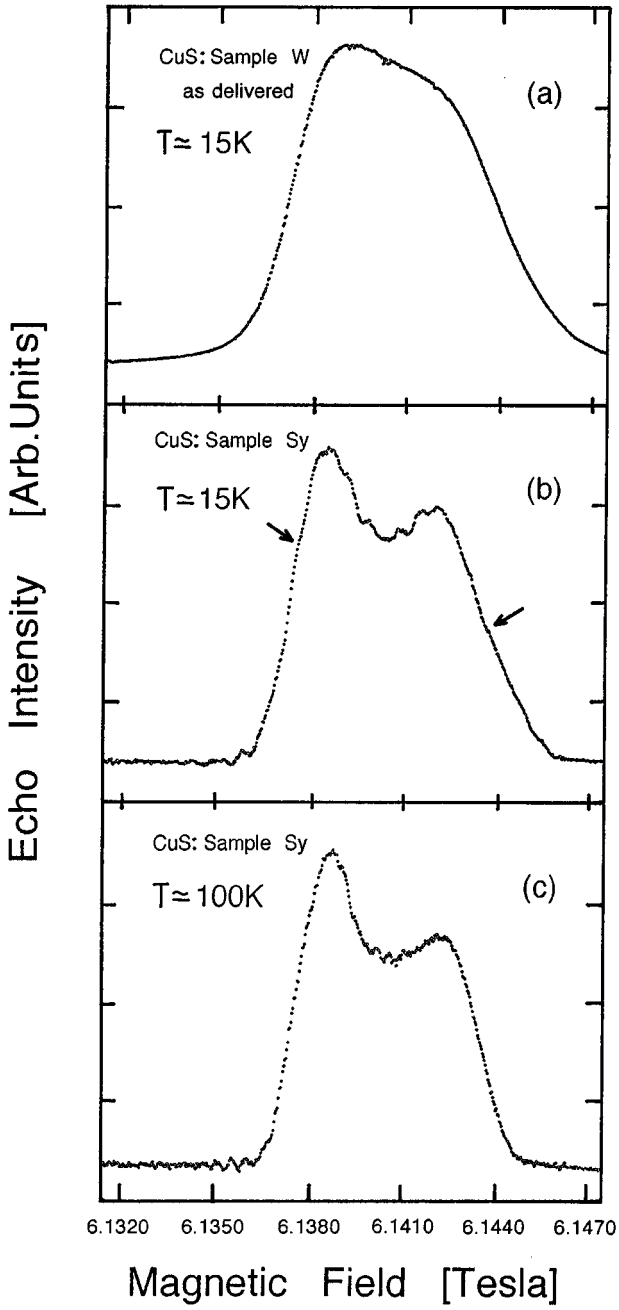

FIG. 5. The central intense peak of echo intensity at the fixed frequency 71 MHz, as a function of magnetic field. (a) The sample *W*, at 15 K. (b) The sample Sy, at 15 K, where the shoulder splittings are indicated by arrows. (c) The sample Sy at 100 K.

Fig. 9. This is not the case of second-order quadrupolar splitting. The second-order quadrupole splittings change as $1/H$. It is considered, therefore, that the exchange of intensities between 6 and 3 T is due to the gathering of dipolar broadened lines.

D. ^{63}Cu NMR: Magnetic-field dependence and assignment of resonance lines

As shown in Fig. 4, the whole resonance envelope of ^{63}Cu NMR includes satellites around the central intense peak, denoted by C. This suggests that there exist first-

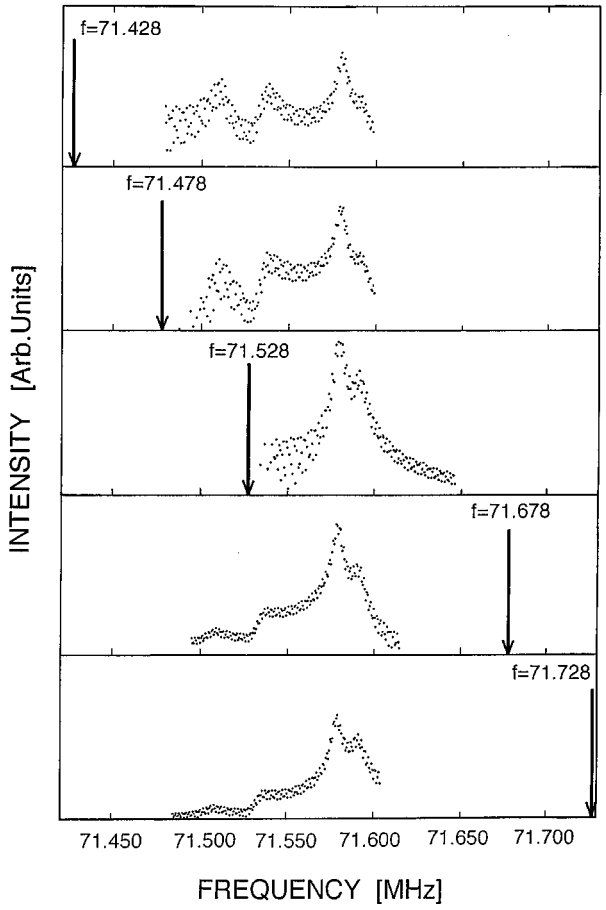

FIG. 6. Power spectra derived from fast Fourier transform (FFT) of free-induction decay (FID) for the sample Sy, at 15 K. The excitation by 90° pulse at frequencies near the resonance has been applied. The positions of excitation frequency are shown by arrow. More than 2000 signals have been accumulated.

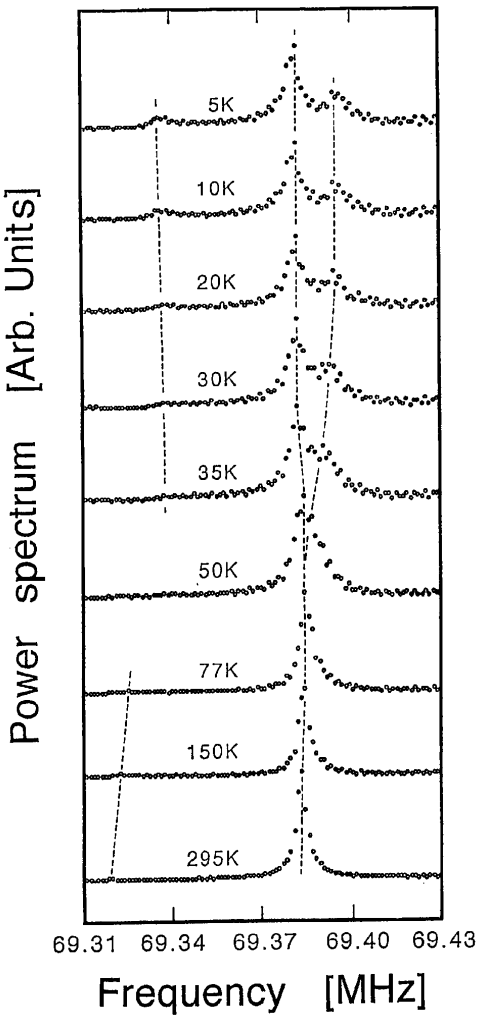

FIG. 7. Power spectra derived from FFT of FID for the sample Sy at various temperatures. The splitting due to crystalline deformation occurs below 50 K.

and/or second-order quadrupole effects.[14] It is known that the first-order quadrupole effect is not affected by the applied magnetic field, provided that the asymmetry parameter $\eta = 0$ holds, while the second-order quadrupole effect depends inversely on the applied magnetic field. Therefore, we can distinguish between the first-order and the second-order quadrupole effects by the measurement of magnetic-field dependence on the resonance splittings.

The details of echo intensity as a function of magnetic field are shown in Fig. 10(a) taken at 60 K, and Fig. 10(b) taken at 15 K. In both Figs. 10(a) and 10(b), the peaks C are so high that the tops of peaks are out of scale. The whole envelope of resonance is shown in the squares inserted in Figs. 10(a) and 10(b). In these figures, the splittings of satellites A_1 and A_2 from the central peak C increase with the decreasing field. The inverse field dependence of splittings of A_1 and A_2 is shown in Fig. 10. The method used by Segel and Creel[15] and Takigawa *et al.*[16] has been adopted for the analysis of satellites A_1 and A_2, based on the second-order quadrupole effect. In Fig. 11, abscissas denote the inverse square of resonance frequency and the vertical axes denote the effective gyromagnetic ratio, γ_{eff}. The dotted straight lines in Fig. 11 indicate that the satellites A_1 and A_2 are due to the splitting of the second-order quadrupole effect (m

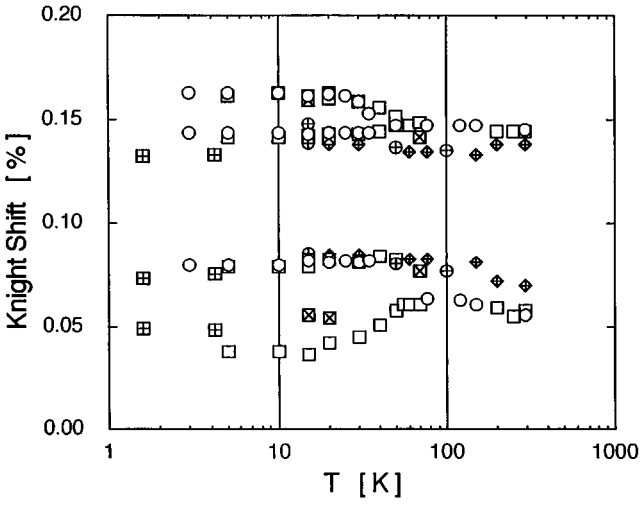

FIG. 8. Temperature dependence of Knight shifts for the central intense peak of the sample Sy shown in Figs. 4, 5, and 6. Zero shift is taken for the resonance of ^{63}Cu in CuBr. Plots are taken from the many experimental runs.

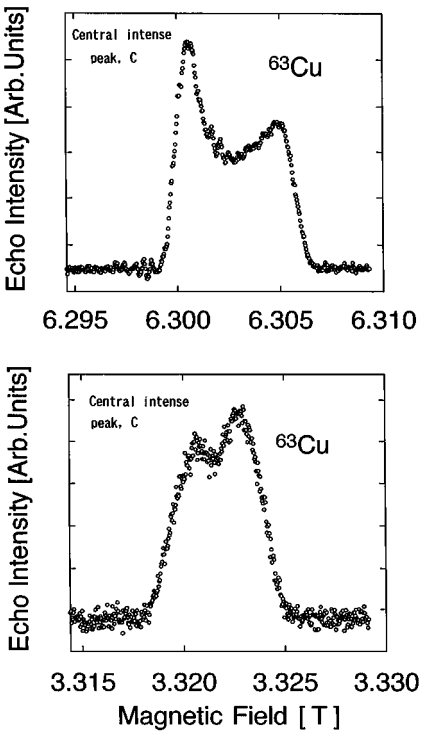

FIG. 9. The profiles of central intense peak C under the different magnetic fields at the room temperature. The more intense peak under the higher field goes to the less intense peak under the lower field.

$=1/2\rightarrow -1/2$), and that the extrapolations of dotted lines to the vertical axis give negative Knight shifts of -0.57% for above 60 K, and -1.4% for below 15 K.

If we assume that the A_1 and A_2 satellites are due to the second-order quadrupole effect between the Cu(1) nucleus and its surrounding EFG, it is concluded that the negative Knight shift is originated by Cu(1)-S bondings, and that there exists the mixing of the d electron of the Cu(1) atom into the conduction band formed by the Cu(1)-S plane. The nuclear quadrupole coupling frequency, $\nu_{1/2\rightarrow -1/2}$ for Cu(1) is estimated to be 14.2 MHz at the room temperature, and 14.5 MHz at 15 K.

The satellites B_1, B_2, D_1, and D_2 are independent of the field variation, as shown in Figs. 10(a) and 10(b). It is considered that the satellite D_1 is an opposite edge of the satellite B_2, and D_2 that of B_1. Therefore, it is evident that these are due to the first-order quadrupole effect. Following the assignment of the first-order quadrupole coupling between Cu(2) and its surrounding EFG, the quadrupole frequency $\nu_{1/2\rightarrow -1/2}$ for Cu(2) is estimated to 1.0 MHz at the room temperature, and 1.8 MHz at 15 K.

In the present work, the powdered sample Sy has been used, therefore, the asymmetry parameter η of EFG for both Cu(1) and Cu(2) nuclei can be estimated when both the splitting peak and shoulder are observable. Only in the cases of 70.6 and 64 MHz shown in Fig. 10(b), have we observed D_1. D_2 is observable in the case of 64 MHz. η for Cu(2) is estimated 0.50–0.55 from the D_1 and D_2 below 50 K.

If there is axial symmetry of EFG's at the temperature above 55 K, asymmetry parameters $\eta=0$ may be considered

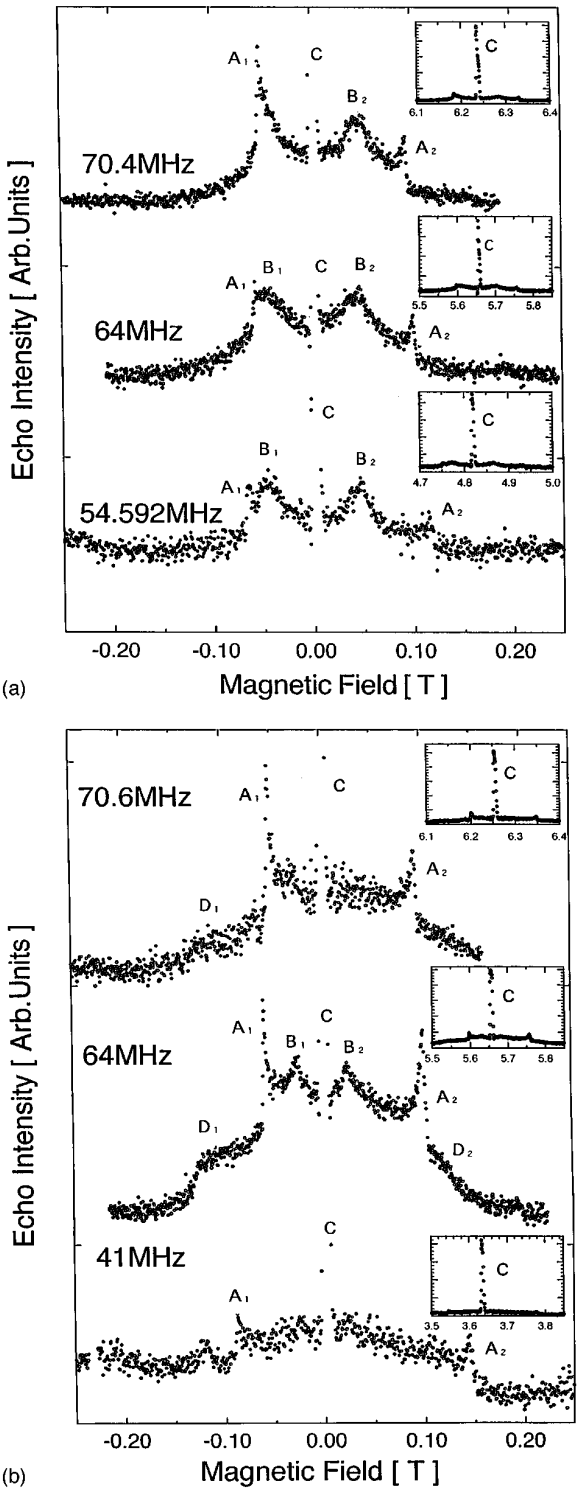

FIG. 10. Echo-intensity profiles as a function of magnetic field. The magnetic field of central intense peak is taken as the center of field. Insets show the total envelope of resonance including the top of C peak. (a) at 60 K. (b) at 15 K.

for Cu(2). The parameters are modified by the crystalline distortion in the region below 50 K. It is considered that the appearances of D_1 and D_2 at temperatures below 15 K, may be due to the change of parameter $\eta=0\rightarrow\eta\neq 0$. In the region below 50 K, $\eta=0.5$ is estimated for Cu(2), while it is hard to estimate the η definitely from the present results for

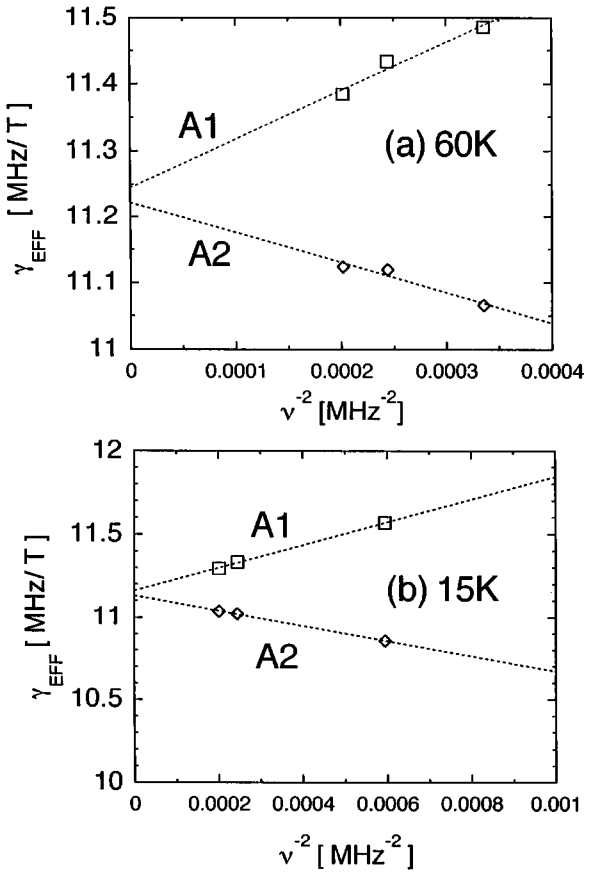

FIG. 11. Effective r of A_1 and A_2 satellites as a function of ν^2. This figure shows that the satellites A_1 and A_2 are due to the splitting basing on the second-order quadrupole effect. (a) at 60 K. (b) at 15 K.

Cu(1). The summary of assignments and estimated $\nu_{1/2\rightarrow -1/2}$ are given in Table II.

E. Spin-lattice relaxation time T_1

An analytic tool for understanding the electronic structure in the sample is a theoretical relationship between Knight shift k and nuclear-spin-lattice-relaxation time T_1, known as the Korringa relation[17,18] $k^2T_1T=$const.

The T_1 results are shown in Fig. 12, where relaxation rate $1/T_1$ of the central intense peak [open circles (○) and triangles (△)] and those of A_1 and A_2 satellites [asterisk (*) and crosses (+)] are plotted as a function of temperatures. As shown in Fig. 12, the relaxation rates, $1/T$, of the central intense peak are linearly proportional to temperatures showing the metallic character. These results are in accordance with the temperature-independent behavior of Knight shift shown in Fig. 8. The T_1's of B_1 and B_2 satellites were nearly equal to those of the central intense peak C. This fact also supports the assignment that B_1 and B_2 satellites are due to the first-order quadrupole effect for C peak.

A particular metallic character of relaxation has been observed in the measurement for the A_1 and A_2 satellites at 15 K. The T_1 of the A_1 satellite is extremely short 3.9 ms (asterisk in Fig. 12), and that of A_2 is 32 ms (cross in Fig. 12). Assuming certain asymmetry parameters for EFG of Cu(1)

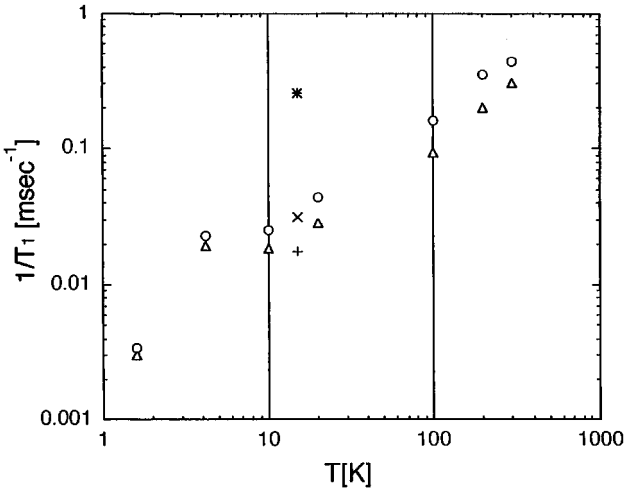

FIG. 12. Spin-lattice relaxation rate $1/T_1$ as a function of temperature. The circles (○) and triangles (△) are for the central intense peak. The asterisk (*) and cross (+) are for the satellites due to the second-order quadrupole effect.

nuclei, the A_1 satellite corresponds to the peak at the angle $\theta=90°$ and A_2 at the angle $\theta=41.8°$ of the second-order quadrupolar splitting. Therefore, the T_1 of the Cu(1) nuclei suggest it to be anisotropic and a metallic one.

The extremely short T_1 might be observed in the case of the magnetic field applied in a direction perpendicular to the crystalline c axis. The direction is parallel to the plane formed by the Cu(1)-S bonds.

IV. DISCUSSIONS

At the present stage, we assigned the shifts observed in ^{63}Cu NMR to a Knight shift. This is based on the electric conductivity[6,13,19,20] and the almost temperature-independent paramagnetic susceptibility[6,13] observed in the substance. These results show the metallic character over the range between T_c and room temperature. The assignment has also been supported by the short relaxation time of echo signals. No change of echo signals has been observed with the repetition of pulse sequence longer than 400 ms at temperature down to 1.7 K.

As mentioned in the foregoing section, Cu(1) nuclei are placed in the plane triangularly coordinated by S atoms, while Cu(2) nuclei are tetrahedrally coordinated by S atoms. Therefore, the EFG surrounding Cu(2) has nearly spherical symmetry or a small coupling of the quadrupole effect, while the EFG for Cu(1) should relatively be larger in the crystalline state. Two sorts of bond length are reported for Cu(2)-S, which are 2.28 and 2.33 Å. These lengths anticipate a distortion from the spherical symmetry around Cu(2) nuclei. The distortion takes place even at room temperature. This may be the reason for the doublet splitting of the central intense peak C, and the doublet goes to a quadruplet in the region below 50 K. It is presumed, therefore, that there are two different sites of Cu(2) at the temperature above 55 K, and four sites of Cu(2) at the temperature below 50 K.

There have been observed some different relaxation behaviors between the peaks assigned to Cu(2) atoms and Cu(1) satellites. The observed results suggest that the metal-

TABLE II. Summary of ^{63}Cu NMR assignments.

Resonance line	Assignment	$\nu_{1/2\rightarrow -1/2}$ at $T=60$ K	$\nu_{1/2\rightarrow -1/2}$ at $T=15$ K	Knight shift, k, %
Satellite A_1, A_2	Cu(1) planar (trigonal)	Second order[b] 14.2 MHz	Second order[b] 14.5 MHz	Negative -0.57(60 K) -1.4(15 K)
Satellite B_1, B_2	Cu(2) tetrahedral	First order[a] 1.0 MHz	First order[a] 1.8 MHz	
Central intense peak, C,	Cu(2) tetrahedral	First order[a] doublet	First order[a] quadruplet	0.04∼0.16
Satellite D_1, D_2	Cu(2) tetrahedral	Not observed	Observed Another edge of B_1, B_2	

a and b mean first- and second-order quadrupole interactions, respectively.

lic character is larger in the plane formed by Cu(1)-S triangular bonds than that formed by Cu(2)-S tetrahedral bonding. If the metallic character of the Cu(1)-S bond in the plane triangularly coordinated by S atoms is hypothetically larger than that of the Cu(2)-S bond, the larger quadrupole interaction occurs in the Cu(1) nuclei, because of the EFG difference between Cu(1) and Cu(2).

The observed values of the ^{63}Cu Knight shift for the central C peak are so small compared to those of ^{63}Cu in copper-oxide superconductors, while those for satellites A_1 and A_2 are particularly negative. The latter seems to be one of the important differences between Cu-S and Cu-O bonds.

Up until now, a number of measurements have been done for the Knight shift K of ^{63}Cu in the high-T_c copper-oxide superconductors. The studies reveal that the antiferromagnetic coupling in the substance plays a key role in the appearance of high-T_c superconductivity, and that such couplings are reflected on the spin susceptibility and K in the normal-state region.

For instance, K's of Cu(I) and Cu(II) in $YBa_2Cu_3O_{6.98}$ ($T_c=93$ K) are larger than about 0.5%, and independent of temperature in the region above T_c, while those for $YBa_2Cu_3O_{6.48}$ ($T_c=59$ K) have a temperature dependence. These K behaviors have been discussed by many authors[16,21,22] from the viewpoint of the spin antiferromagnetic coupling, which are characteristic in the high-T_c copper-oxide superconductors.

If the coupling, therefore, plays a key role in changing T_c, it would be suggestive to compare K's measured in CuS with those in the high-T_c superconductors. K's of Cu(2) in CuS, which are assigned to the intense central peak C are 0.04–0.16 % and are nearly independent of temperature as shown in Fig. 8. Furthermore, it seems that K of Cu(1) is also independent of temperature from the results shown in Figs. 9(a) and 9(b). Unfortunately, there is no evidence of magnetic ordering about Cu_2S, $Cu_{1.96}S$, and $Cu_{1.8}S$. These compounds are p-type semiconductors. CuS and CuS_2 are nearly metallic and superconductors, although an anomalous transition in CuS_2 has been reported,[23] suggesting a possible antiferromagnetic ordering. It is important to clarify the magnetic characters in these various sulfuric compounds and also to seek the temperature-dependent K caused by the antiferromagnetic spin coupling. These efforts might be related to increasing T_c.

The experiments for the sample Sy have been done below T_c under the magnetic field near 6 T, but no essential change to those for above T_c has been observed because the applied field is larger than the critical field of CuS. The resonance experiment under zero field is now in preparation. Further magnetic investigations with the single crystal of CuS are also preferable to obtain more detailed information.

ACKNOWLEDGMENTS

The ^{63}Cu NMR work was done with the pulsed NMR apparatus of the Laboratory for Development Research of Advanced Materials Research, Institute for Materials Research, Tohoku University. The authors of Toin University are grateful to the Institute for Materials Research, Tohoku University, for financial support.

*Present address: Watkins-Johnson International Japan K.K.
†Present address: Shin-nihon Keiso Co. Ltd. Japan.

[1] W. Meissner, Z. Phys. **58**, 570 (1929).
[2] W. Buckel and R. Hilsh, Z. Phys. **128**, 324 (1950).
[3] J. G. Bednorz and K. Muller, Z. Phys. B **64**, 189 (1986).
[4] *Powder Diffraction File*, edited by L. G. Berry (Joint Committee on Powder Diffraction Standards, Swarthmore, Pennsylvania, 1980), Vol. PD1S-10iRB, p. 87.
[5] H. T. Evans, Jr., and J. A. Konnert, Am. Mineral. **61**, 996 (1976), and references cited therein.
[6] H. Fjellvag, F. Gronvold, S. Stolen, A. F. Andresen, R. Muller-Kafer, and A. Simon, Z. Kristallogr. **184**, 111 (1988), and references cited therein.
[7] M. Isino and E. Kanda, J. Phys. Soc. Jpn. **35**, 1257 (1973).
[8] E. F. Westrum, Jr., S. Stolen, and F. Gronvold, J. Chem. Thermodyn. **19**, 1199 (1987).
[9] J. R. Clem, in *Magnetic Susceptibility of Superconductors and other Spin Systems*, edited by R. A. Hein, T. L. Francavilla, and D. H. Liebenberg (Plenum, New York, 1991), p. 177.
[10] A. K. Khoder and M. Couach, *Magnetic Susceptibility of Superconductors and other Spin Systems* (Ref. 9), p. 213.
[11] E. Maxwell and M. Strongin, Phys. Rev. Lett. **10**, 212 (1963).

[12] T. Ishida and H. Mazaki, Phys. Rev. B **20**, 131 (1979); J. Appl. Phys. **52**, 6798 (1981).
[13] H. Nozaki, K. Shibata, and N. Ohhashi, J. Solid State Chem. **91**, 306 (1991).
[14] M. H. Cohen and F. Reif, in *Solid State Physics: Advances in Research and Applications*, edited by F. Seitz and D. Turnbull (Academic, New York, 1957), Vol. 5, p. 321, and references cited therein.
[15] S. L. Segel and R. B. Creel, Can. J. Phys. **48**, 2673 (1970).
[16] M. Takigawa, P. C. Hammel, R. H. Heffuer, Z. Fisk, J. L. Smith, and R. B. Schwarz, Phys. Rev. B **39**, 300 (1989).
[17] J. Korringa, Physica **16**, 601 (1959).
[18] G. C. Carter, L. H. Bennett, and D. J. Kahan, *Metallic Shifts in NMR* (Pergamon, New York, 1977), Pt. 1.
[19] K. Okamoto, Jpn. J. Appl. Phys. **8**, 718 (1969).
[20] S. H. Saito and H. Nakamaru (unpublished).
[21] F. Mila and T. M. Rice, Phys. Rev. B **40**, 11 382 (1989).
[22] H. Monien, D. Pines, and M. Takigawa, Phys. Rev. B **43**, 258 (1991).
[23] F. Gautier, G. Krill, P. Panissod, and C. Robert, J. Phys. C **7**, L170 (1974).